Specific Ion Effects on Interfacial Water Structure near Macromolecules

ARTICLE *in* JOURNAL OF THE AMERICAN CHEMICAL SOCIETY · OCTOBER 2007

Impact Factor: 12.11 · DOI: 10.1021/ja073869r · Source: PubMed

4 AUTHORS, INCLUDING:

Sho Kataoka
National Institute of Advanced Industrial Sci…
50 PUBLICATIONS **1,295** CITATIONS

SEE PROFILE

J|A|C|S
ARTICLES
Published on Web 09/19/2007

Specific Ion Effects on Interfacial Water Structure near Macromolecules

Xin Chen, Tinglu Yang, Sho Kataoka, and Paul S. Cremer*

Contribution from the Department of Chemistry, Texas A&M University, College Station, Texas 77843

Received May 29, 2007; E-mail: cremer@mail.chem.tamu.edu

Abstract: We investigated specific ion effects on interfacial water structure next to macromolecules with vibrational sum frequency spectroscopy (VSFS). Poly-(*N*-isopropylacrylamide) was adsorbed at the air/water interface for this purpose. It was found that the presence of salt in the subphase could induce the reorganization of water adjacent to the macromolecule and that the changes depended greatly on the specific identity and concentration of the salt employed. Ranked by their propensity to orient interfacial water molecules, sodium salts could be placed in the following order: NaSCN > $NaClO_4$ > NaI > $NaNO_3$ ≈ NaBr > NaCl > pure water ≈ NaF ≈ Na_2SO_4. This ordering is a Hofmeister series. On the other hand, varying the identity of the cation exhibited virtually no effect. We also showed that the oscillator strength in the OH stretch region was linearly related to changes in the surface potential caused by anion adsorption. This fact allowed binding isotherms to be abstracted from the VSFS data. Such results offer direct evidence that interfacial water structure can be predominantly the consequence of macromolecule−ion interactions.

Introduction

The Hofmeister series,[1−5] was first constructed almost 120 years ago to characterize the ability of salts to precipitate proteins from aqueous solution.[1] The qualitative order of the anions is

$$SO_4^{2-} > F^- > Cl^- > NO_3^- > Br^- > I^- > ClO_4^- > SCN^-$$

The ions at the right end of the series are referred to as chaotropes and usually act to salt protein molecules into solution, while the ions on the left are called kosmotropes and cause proteins to salt-out of solution. The chloride ion typically designates the dividing line between the two types of behavior. The importance of the Hofmeister series goes well beyond the solubility of proteins. Indeed, it plays a critical role in a wide variety of chemical and physical phenomena.[2−5] Despite its long history and wide impact, a molecular level understanding of this series is still far from complete. The Hofmeister effect was originally explained by the capacity of various ions to "make" or "break" bulk water structure.[2−5] This idea has been challenged, however, by many recent experimental[6−8] and theoretical[9−11] studies. In fact, those investigations have clearly showed that the properties of bulk water are not significantly perturbed by ions dissolved in solution.

The Hofmeister effect can be treated as an interfacial phenomenon.[2−4,12] Specifically, the direct interactions of ions with the macromolecule/aqueous interface should be of central significance. Interfacial water structure plays a key role in the thermodynamic and kinetic properties of macromolecules and biomacromolecules dissolved in aqueous solution.[13,14] Contrary to the conventional belief that ions are absent from surfaces and interfaces, recent experimental and theoretical studies have proven that ions, particularly anions, can be present and even enriched at the top most layer of surfaces and interfaces.[8,15−23] This raises some important questions. First, how is interfacial water structure affected by the presence of Hofmeister ions?

(1) Hofmeister, F. *Arch. Exp. Pathol. Pharmakol.* **1888**, *24*, 247−260.
(2) Collins, K. D.; Washabaugh, M. W. *Q. Rev. Biophys.* **1985**, *18*, 323−422.
(3) Cacace, M. G.; Landau, E. M.; Ramsden, J. J. *Q. Rev. Biophys.* **1997**, *30*, 241−277.
(4) Clarke, R. J.; Lupfert, C. *Biophys. J.* **1999**, *76*, 2614−2624.
(5) Kunz, W.; Lo Nostro, P.; Ninham, B. W. *Curr. Opin. Coll. Int. Sci.* **2004**, *9*, 1−18.
(6) Omta, A. W.; Kropman, M. F.; Woutersen, S.; Bakker, H. J. *Science* **2003**, *301*, 347−349.
(7) Batchelor, J. D.; Olteanu, A.; Tripathy, A.; Pielak, G. J. *J. Am. Chem. Soc.* **2004**, *126*, 1958−1961.
(8) Gurau, M. C.; Lim, S. M.; Castellana, E. T.; Albertorio, F.; Kataoka, S.; Cremer, P. S. *J. Am. Chem. Soc.* **2004**, *126*, 10522−10523.
(9) Bostrom, M.; Williams, D. R. M.; Ninham, B. W. *Phys. Rev. Lett.* **2001**, *87*, 168103.
(10) Bostrom, M.; Williams, D. R. M.; Ninham, B. W. *Biophys. J.* **2003**, *85*, 686−694.
(11) Bostrom, V.; Kunz, W.; Ninham, B. W. *Langmuir* **2005**, *21*, 2619−2623.
(12) Courtenay, E. S.; Capp, M. W.; Record, M. T. *Protein Sci.* **2001**, *10*, 2485−2497.
(13) Bagchi, B. *Chem. Rev.* **2005**, *105*, 3197−3219.
(14) Benjamin, I. *Chem. Rev.* **1996**, *96*, 1449−1475.
(15) Jungwirth, P.; Tobias, D. J. *J. Phys. Chem. B* **2002**, *106*, 6361−6373.
(16) Jungwirth, P.; Tobias, D. J. *J. Phys. Chem. B* **2001**, *105*, 10468−10472.
(17) Knipping, E. M.; Lakin, M. J.; Foster, K. L.; Jungwirth, P.; Tobias, D. J.; Gerber, R. B.; Dabdub, D.; Finlayson-Pitts, B. J. *Science* **2000**, *288*, 301−306.
(18) Petersen, P. B.; Saykally, R. J. *Chem. Phys. Lett.* **2004**, *397*, 51−55.
(19) Ghosal, S.; Hemminger, J. C.; Bluhm, H.; Mun, B. S.; Hebenstreit, E. L. D.; Ketteler, G.; Ogletree, D. F.; Requejo, F. G.; Salmeron, M. *Science* **2005**, *307*, 563−566.
(20) Jungwirth, P.; Tobias, D. J. *Chem. Rev.* **2006**, *106*, 1259−1281.
(21) Gopalakrishnan, S.; Liu, D. F.; Allen, H. C.; Kuo, M.; Shultz, M. J. *Chem. Rev.* **2006**, *106*, 1155−1175.
(22) Pegram, L. M.; Record, M. T. *Proc. Natl. Acad. Sci. U.S.A.* **2006**, *103*, 14278−14281.
(23) Liu, D. F.; Ma, G.; Levering, L. M.; Allen, H. C. *J. Phys. Chem. B* **2004**, *108*, 2252−2260.

10.1021/ja073869r CCC: $37.00

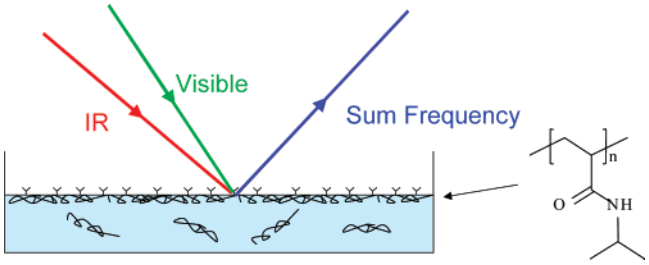

Figure 1. Schematic diagram of the experimental setup for using VSFS to monitor PNIPAM at the air/water interface. The structure of PNIPAM is also shown.

Second, how do these interactions contribute to the overall Hofmeister effect?

An attractive technique for investigating interfacial water and polymer structure is vibrational sum frequency spectroscopy (VSFS).[24−26] VSFS is a second-order nonlinear optical spectroscopy, which is inherently surface/interface specific. The technique has proven to be a very powerful method for investigating the molecular level details of interfaces. Numerous VSFS studies have focused on interfacial solvent molecules and/or species adsorbed at interfaces.[21,26−28] One topic that has received a particularly large amount of attention involves polymers and proteins adsorbed at solution interfaces.[28−32] Many water-soluble macromolecules are surface active and can adsorb at the air/water interface from solution with their hydrophobic moieties well-aligned into the gas phase. Such alignment can be easily monitored by measuring the sum frequency response in the CH-stretch range. Moreover, the OH-stretch range of the VSFS spectrum can report on interfacial water structure next to the adsorbed macromolecules. The interference between the OH and CH features provides information about the relative orientation of these oscillators.[33−36]

Despite the potential utility of VSFS for monitoring adsorbed polymers and proteins at interfaces, no previous VSFS studies, to the best of our knowledge, have focused on specific ion effects in such systems. In this work, we investigate the effects of Hofmeister anions on a polymer, poly-(*N*-isopropylacrylamide) (PNIPAM), and the water structure next to it (Figure 1). Specific ion effects can be monitored by VSFS as the salt in the aqueous subphase is varied. PNIPAM is an attractive molecule for such investigations for several reasons. It contains both isopropyl groups, which are hydrophobic, and amide moieties, which are more hydrophilic.[37,38] Similar to many other polymers and proteins, PNIPAM, can be adsorbed to the air/water interface from solution to form a Gibbs monolayer which is well suited for VSFS studies. A unique property of PNIPAM is its lower critical solution temperature (LCST). This means that PNIPAM will precipitate out from aqueous solution above a specific temperature (∼31 °C in pure water).[37,38] This phenomenon is very similar to the cold denaturation/renaturation phase transition of proteins. Additionally, the LCST of PNIPAM is known to be very sensitive to the identity and concentration of co-dissolved salts in solution.[37−41]

Results from the current VSFS studies clearly show that the water structure at the air/PNIPAM/aqueous interface is very sensitive to the salts present in the subphase. In fact, the extent of water orientation closely followed the Hofmeister series for the anions. More chaotropic ions generated stronger water orientation. On the other hand, the CH-stretch region was unaffected by the nature and concentration of the salt in the subphase. This indicated that the surface concentration and orientation of PNIPAM remained nearly unchanged in all the experiments that were conducted. The cations were varied as well. In contrast to the anions, the specific nature of the cations showed little if any influence. This observation could be attributed to the preferential interactions of the anions with the polymer. Furthermore, the concentration dependent effects of the various anions could be quantitatively modeled by employing Gouy−Chapman−Stern theory. The equilibrium dissociation constants for anion adsorption could, therefore, be determined. The values of the dissociation constants for the anions with PINPAM were found to be 0.15 M for perchlorate, 0.19 M for thiocyanate, 0.50 M for iodide, 3.8 M for nitrate, 4.0 M for bromide, and 15 M for chloride.

Materials and Methods

Materials. All inorganic salts (from Aldrich, MO and Fisher, NJ) were used as received. PNIPAM was synthesized by free radical polymerization from its monomer following procedures described previously.[37] The sample had a molecular weight of 1.70×10^5 g/mol and a polydispersity of 1.32.[37] Aqueous solutions were prepared from purified water with a minimum resistivity of 18.1 MΩ·cm (NANOpure Ultrapure Water System, Barnstead, Dubuque, IA). When D_2O solutions were employed instead, the heavy water was obtained from Cambridge Isotope Laboratories (Andover, MA). All solutions were prepared by addition of the appropriate salt to purified water or D_2O. No buffer was used to control the pH. While it would have been possible to precisely control the pH of these solutions through the addition of buffers, this would have necessitated the use of additional salts. Most of the anions explored herein make strong acids, so the solutions of the corresponding sodium salts have nearly neutral pH values. The most important exception to this is NaF, which causes its saturated salt solution to be basic (pH ≈ 10.6).

We wished to determine if modulating the pH of the bulk solution would have an effect on VSFS spectra at the interface. Therefore, experiments were performed at pH 3.0 and 11.0. The acidic and basic solutions were prepared by adding HCl and NaOH, respectively, to purified water with no additional salts. The spectra in these cases were identical within experimental error to the data from pure water (see Supporting Information, Figure S1). These results demonstrated that neither PNPAM nor the interfacial water structure was significantly affected. Indeed, PNIPAM has no titratable groups in this pH range.

(24) Shen, Y. R. *The Principles of Nonlinear Optics*; Wiley: New York, 1984.
(25) Hirose, C.; Akamatsu, N.; Domen, K. *Appl. Spectrosc.* **1992**, *46*, 1051−1072.
(26) Richmond, G. L. *Chem. Rev.* **2002**, *102*, 2693−2724.
(27) Shen, Y. R.; Ostroverkhov, V. *Chem. Rev.* **2006**, *106*, 1140−1154.
(28) Chen, X. Y.; Clarke, M. L.; Wang, J.; Chen, Z. *Inter. J. Mod. Phys. B* **2005**, *19*, 691−713.
(29) Kim, G.; Gurau, M.; Kim, J.; Cremer, P. S. *Langmuir* **2002**, *18*, 2807−2811.
(30) Wang, J.; Buck, S. M.; Chen, Z. *J. Phys. Chem. B* **2002**, *106*, 11666−11672.
(31) Wang, J.; Clarke, M. L.; Zhang, Y. B.; Chen, X. Y.; Chen, Z. *Langmuir* **2003**, *19*, 7862−7866.
(32) Kim, J.; Somorjai, G. A. *J. Am. Chem. Soc.* **2003**, *125*, 3150−3158.
(33) Gragson, D. E.; McCarty, B. M.; Richmond, G. L. *J. Phys. Chem.* **1996**, *100*, 14272−14275.
(34) Gragson, D. E.; McCarty, B. M.; Richmond, G. L. *J. Am. Chem. Soc.* **1997**, *119*, 6144−6152.
(35) Gragson, D. E.; Richmond, G. L. *J. Phys. Chem. B* **1998**, *102*, 3847−3861.
(36) Gragson, D. E.; Richmond, G. L. *J. Am. Chem. Soc.* **1998**, *120*, 366−375.
(37) Zhang, Y. J.; Furyk, S.; Bergbreiter, D. E.; Cremer, P. S. *J. Am. Chem. Soc.* **2005**, *127*, 14505−14510.
(38) Schild, H. G. *Prog. Polym. Sci.* **1992**, *17*, 163−249.
(39) Dhara, D.; Chatterji, P. R. *J. Macromol. Sci. Rev. Macromol. Chem. Phys.* **2000**, *C40*, 51−68.
(40) Suwa, K.; Yamamoto, K.; Akashi, M.; Takano, K.; Tanaka, N.; Kunugi, S. *Colloid Polym. Sci.* **1998**, *276*, 529−533.
(41) Freitag, R.; Garret-Flaudy, F. *Langmuir* **2002**, *18*, 3434−3440.

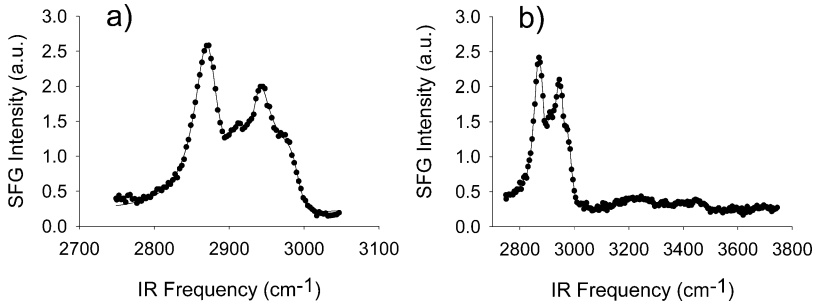

Figure 2. VSFS spectrum of PNIPAM at (a) the D_2O/air interface and (b) the H_2O/air interface.

Vibrational Sum Frequency Spectroscopy. Our VSFS system has been described in detail elsewhere.[29,42,43] Briefly, the visible and infrared inputs were generated by an optical parametric generator/amplifier (OPG/OPA) stage pumped with a Nd:YAG laser, which generated a 50 mJ, 17 ps pulse at 1064 nm. The frequency of the infrared beam could be tuned between 2000 and 4000 cm^{-1}. The system supplied ~0.7 mJ per pulse near 3000 cm^{-1}. The 532 nm beam was adjusted to ~1 mJ per pulse at the sample surface.

To perform VSFS experiments on PNIPAM monolayers, a 35 mL salt solution containing 0.006 mg/mL PNIPAM was poured into a small Langmuir trough (Model 601M, Nima, U.K.), which was held at a constant temperature of 12 °C. This concentration was more than sufficient to form a saturated Gibbs monolayer. In fact, raising the concentration by 1 order of magnitude led to no observable changes in the VSFS spectra. The visible and infrared beams were spatially and temporally aligned to the air/polymer/aqueous interface of the Langmuir trough and the VSFS signal was collected with a photomultiplier tube (Hamamatsu, Japan). All spectra were recorded with the ssp (s-sum frequency, s-visible, and p-infrared) polarization combination.

The intensity of the sum frequency signal, I_{SFG}, could be modeled using eq 1:

$$I_{SFG} \propto |\chi^{(2)}_{eff}|^2 \bullet I_{vis} \bullet I_{IR} \quad (1)$$

where I_{vis} and I_{IR} are the intensities of the incoming visible and infrared laser beams, respectively. The term $\chi^{(2)}_{eff}$ denotes the effective second-order nonlinear susceptibility, which can be further expressed as

$$\chi^{(2)}_{eff} = \chi^{(2)}_{NR} + \chi^{(2)}_{R} = \chi^{(2)}_{NR} + \sum_q \frac{A_q}{\omega_{IR} - \omega_q + i\Gamma_q} \quad (2)$$

where $\chi^{(2)}_{NR}$ and $\chi^{(2)}_{R}$ are the frequency-independent nonresonant term and the frequency-dependent resonant term, respectively. $\chi^{(2)}_{R}$ of the qth resonant mode is a function of the oscillation strength, A_q, resonant frequency, ω_q, peak width, Γ_q, and the frequency of the input infrared laser beam, ω_{IR}.

The VSFS spectra reported herein were reproduced a minimum of three times over at least a 45 min time period to ensure equilibrium had been achieved. Longer time periods showed no evidence of spectral changes. The spectra have each been normalized to the nonresonant response from a piece of Z-cut crystalline quartz after background subtraction. The normalized spectra were fit to eq 2 by a computer program using MATLAB software. The oscillator strengths, A_q, of the water peaks could thereby be abstracted.

Surface Potential Measurements. Surface potentials measurements on Gibbs monolayers of PNIPAM with various salts in the subphase were measured in a large Langmuir trough (KSV 5000, KSV Instruments Ltd., Helsinki, Finland). This trough was equipped with a Kelvin probe for performing vibrating capacitor measurements.[44,45] In these experiments, the aqueous subphases were prepared in a similar manner to the VSFS experiments. In this case, each measurement was carried out after waiting at least 20 min to stabilize the reading from the Kelvin probe. The surface potential values were determined from the average of 3 to 10 measurements. The absolute values of the surface potential varied from day to day; however, changes in the surface potential as a function of the salt solution were far more consistent over the course of a given day (on average ± 14 mV), and this relative difference stayed consistent from day to day. It is this relative difference that is employed in the current work.

Results

VSFS Spectral Features. VSFS measurements of a Gibbs monolayer of PNIPAM were made on a D_2O subphase (Figure 2a). The spectrum contained four prominent peaks in the CH stretch region (2800 to 3000 cm^{-1}). The positions of the peaks, 2874, 2913, 2939, and 2980 cm^{-1}, were abstracted by fitting the data to eq 2. The 2874 cm^{-1} peak can be assigned to the CH_3 symmetric stretch (r^+) of the isopropyl moiety.[43,46] The 2913 cm^{-1} feature, which was much weaker, is due to the methine stretch of the isopropyl group. The assignments of the other two peaks at 2939 and 2980 cm^{-1} are typically attributed to a Fermi resonance(r^+_{FR}), and the CH_3 asymmetric stretch (r^-), respectively. The features are similar to the VSFS spectrum reported for a thin PNIPAM film cast on a CaF_2 crystal,[47] although the 2913 cm^{-1} peak was assign differently. The intensities and positions of these peaks are strikingly similar to previous studies of Gibbs monolayers of isopropanol on aqueous solutions[43,46] as well as to other analogous systems presenting an isopropyl group.[48,49]

Next, the identical experiment was repeated in H_2O. This time two small additional features near 3200 and 3400 cm^{-1} arose in the VSFS spectrum (Figure 2b). They can be assigned to the OH stretch modes of aligned interfacial water molecules. These peaks are quite weak compared with the features in the CH stretch range. Indeed, PNIPAM does not possess any charged residues, which would help align interfacial water molecules. Similarly weak interfacial water features have been previously observed at the air−water interface in the presence of neutral surfactants and proteins near their isoelectric points.[29,30,33−36]

Effect of Anion Identity. Various sodium salts were introduced into the aqueous subphase to investigate anion effects

(42) Kataoka, S.; Gurau, M. C.; Albertorio, F.; Holden, M. A.; Lim, S. M.; Yang, R. D.; Cremer, P. S. *Langmuir* **2004**, *20*, 1662−1666.
(43) Kataoka, S.; Cremer, P. S. *J. Am. Chem. Soc.* **2006**, *128*, 5516−5522.
(44) Aveyard, R.; Haydon, D. A. *An Introduction to the Principles of Surface Chemistry*; University Press: Cambridge, U.K., 1973.
(45) Adamson, A. W.; Gast, A. P. *Physical Chemistry of Surfaces*; Wiley: New York, 1997.
(46) Lu, R.; Gan, W.; Wu, B. H.; Zhang, Z.; Guo, Y.; Wang, H. F. *J. Phys. Chem. B* **2005**, *109*, 14118−14129.
(47) Cheng, X. H.; Canavan, H. E.; Stein, M. J.; Hull, J. R.; Kweskin, S. J.; Wagner, M. S.; Somorjai, G. A.; Castner, D. G.; Ratner, B. D. *Langmuir* **2005**, *21*, 7833−7841.
(48) Ji, N.; Shen, Y. R. *J. Chem. Phys.* **2004**, *120*, 7107−7112.
(49) Ji, N.; Shen, Y. R. *J. Am. Chem. Soc.* **2004**, *126*, 15008−15009.

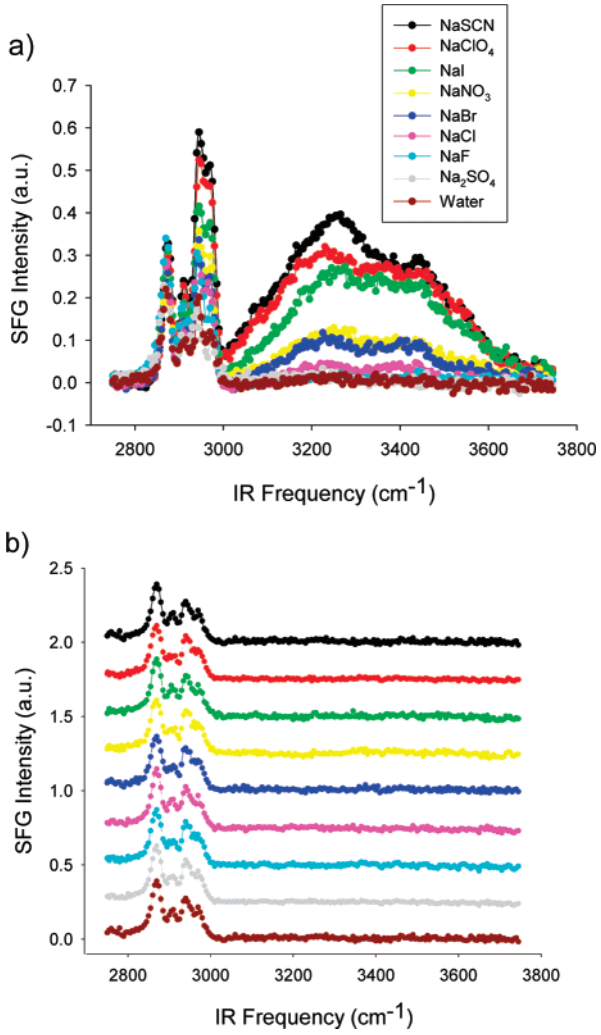

Figure 3. (a) VSFS spectra show specific anion effects on PNIPAM adsorbed at the air/water interface. Each subphase contained 1 M of a given salt as indicated in the legend except for NaF and Na_2SO_4, which are measured with saturated solutions (~0.8 M for both salts). (b) The same experiments repeated with D_2O. The spectra are offset for clarity.

on interfacial water structure in the presence of PNIPAM. The salts included 1 M NaSCN, 1 M $NaClO_4$, 1 M NaI, 1 M $NaNO_3$, 1 M NaBr, and saturated solutions of NaF (~0.8 M) and Na_2SO_4 (~0.8 M). From the VSFS spectra plotted in Figure 3a, it is obvious that the water peaks became more prominent in the presence of chaotropic anions. The sodium salt of the most chaotropic anion, SCN^-, induced the greatest water peak intensity, while the most kosmotropic species, SO_4^{2-}, had almost no influence on the water structure. The OH stretch peak intensities were clearly anion specific and followed the Hofmeister series:

$$SCN^- > ClO_4^- > I^- > NO_3^- \approx Br^- > Cl^- > \text{pure water} \approx F^- \approx SO_4^{2-}$$

The 3200 and 3400 cm^{-1} peaks both followed the series and the fitted values of their oscillator strengths are provided in the Supporting Information (Table S1).

Next, it was necessary to determine if the interfacial polymer concentration was changed by the presence of different aqueous subphases. The VSFS spectra in Figure 3a show apparently different peak heights in the CH stretch range; however, the intensities should not be directly compared because of varying interferences with the OH peaks. To eliminate this interference, the experiments were repeated with D_2O subphases under otherwise identical conditions, as shown in Figure 3b. It can be clearly seen that the peaks in the CH region were unchanged regardless of the anion employed. In fact, the positions and intensities of all the peaks were identical within experimental error to those found without any salt. This clearly demonstrates that salt does not substantially perturb either the concentration or orientation of the isopropyl moieties of PNIPAM at the air/water interface. This lack of change is probably the result of a collective interaction with the vapor phase, whereby the large number of hydrophobic isopropyl side chains keeps PNIPAM's orientation fixed regardless of the specific solution conditions.

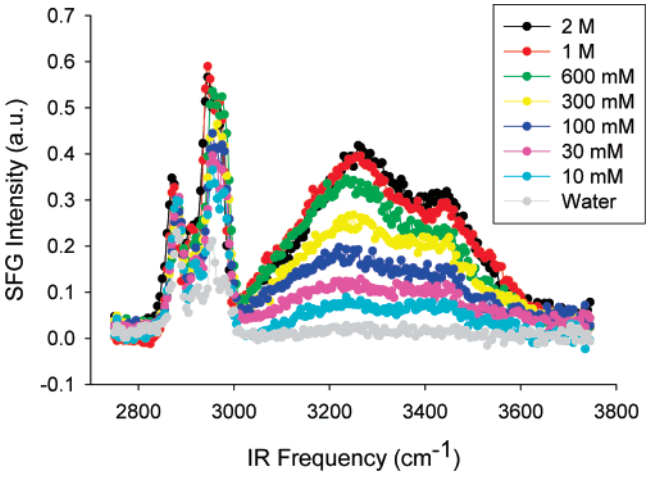

Figure 4. VSFS spectra of the air/PNIPAM/aqueous interface as a function of sodium thiocyanate concentration in the subphase.

Effect of Chaotropic Anion Concentration. The PNIPAM interfaces were further probed by VSFS as a function of salt concentration. The VSFS spectra in Figure 4 show changes in water structure as a function of salt concentration between 0 and 2 M NaSCN. At low NaSCN concentration, the peak intensity in the OH stretch region increased rapidly with increasing salt concentration, but the changes were much more modest above 0.6 M NaSCN. These spectra can be fit with Eqn. 2 and the abstracted oscillator strengths of the 3200 cm^{-1} peak are plotted against NaSCN concentration in Figure 5 (solid circles, ●). The same measurements were repeated for the other Hofmeister salts and these data are also plotted in Figure 5. The oscillator strength of the 3200 cm^{-1} peak was found to increase and then level off in most cases. For the strongest chaotropes, such as thiocyanate and iodide, the oscillator strength increased relatively fast in the low concentration range regime (<100 mM). By contrast, it increased much more slowly for the weaker chaotropes. The shape of curves was quite reminiscent of a Langmuir isotherm and the lines in Figure 5 represent fits to this equation:

$$OS = \frac{B_{max} C/K_{D,app}}{1 + C/K_{D,app}} \quad (3)$$

where OS stands for the oscillator strength of the 3200 cm^{-1} peak and C stands for the chaotropic anion concentration. B_{max} represents the maximum value of OS for a particular ion at infinite concentration. $K_{D,app}$ is the apparent equilibrium dissociation constant. The fits were reasonably good in most cases.

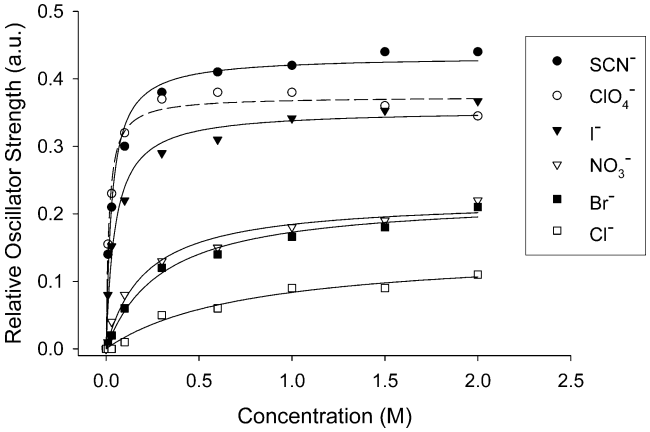

Figure 5. The relative oscillator strength of the 3200 cm^{-1} peak vs anion concentration in the subphase. The lines are Langmuir isotherm fits to the data. The fit for perchlorate is denoted by a dashed line as it is obviously not as good as for the other anions.

Table 1. Dissociation Constants of Anions to PNIPAM

	SCN^-	ClO_4^-	I^-	NO_3^-	Br^-	Cl^-
$K_{D,app}$ (M)	0.031	0.016	0.048	0.20	0.30	0.76
B_{max} (au)	0.43	0.37	0.35	0.22	0.22	0.15
$K_{D,intrinsic}$ (M)	0.19	0.15	0.50	3.8	4.0	15

The abstracted values of $K_{D,app}$ and B_{max} for all the anions are provided in Table 1. The greatest deviation from Langmuir-type behavior was found for perchlorate (Figure 5, open circles, ○). In this case, the oscillator strength rose quickly at low-salt concentration, reached a maximum near 600 mM, and then decreased slightly but steadily at higher concentrations.

Surface Potential. Surface potential measurements were made at the air/PNIPAM/aqueous interface with the same eight salts employed in the VSFS experiments. These measurements were made to determine if changes in the water peaks could be correlated to changes in the potential at the interface. The surface potential of the air/PNIPAM/water interface was ca. −360 mV in the absence of salt in the subphase. Upon addition of the salts, the potential became more negative for the chaotropic salts, but barely changed within experimental error when kosmotropic salts were added to solution. The change in potential with a 1 M concentration of each salt is plotted in Figure 6 , and the numerical values are listed in the Supporting Information (Table S1). Again, the same measurements were performed with only ∼0.8 M NaF and ∼0.8 M Na_2SO_4.

As can be seen, SCN^- had the greatest ability to attenuate the surface potential and this propensity decreased with the other anions according to the Hofmeister series. A linear correlation could be established between the measured surface potential and the abstracted oscillator strength of the water peaks (Figure 6, solid circles, ●). This remarkable result suggests that changes in the surface potential were directly related to changes in the OH-stretch region of the VSFS spectra. The surface potential was also directly measured for NaSCN and $NaClO_4$ at various salt concentrations. The numerical values are provided in Table S2 of the Supporting Information. These values are also plotted in Figure 6 and show the same linear correlation to the oscillator strength of the 3200 cm^{-1} peak (open circles, ○, for NaSCN and open triangles, △, for $NaClO_4$).

It should be noted that similar correlations between nonlinear optical signals and surface potential have previously been found

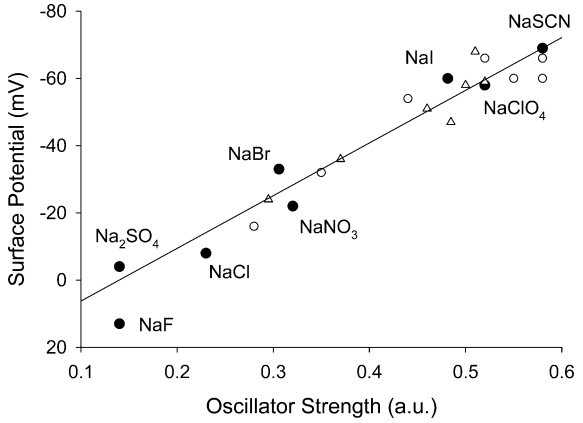

Figure 6. Correlation between the surface potential and the oscillator strength for the 3200 cm^{-1} peak. The solid circles are 1 M salt concentrations of the Hofmeister salts except for sulfate and fluoride which were ∼0.8 M. The open circles and open triangles represent various concentrations of NaSCN and $NaClO_4$, respectively. The average error bar for each data point is ±14 mV.

at aqueous interfaces in second harmonic generation (SHG) studies,[50−52] although they are less common in SFG studies.[33−36] This type of correlation may be due to a $\chi^{(3)}$ effect or simply caused by the charge induced alignment of water.[33−36] Next, it should be noted that high quality data for surface potential versus salt concentration could only be obtained for strong chaotropes. The reason stemmed from signal-to-noise limitations of the vibrating capacitor technique.[45] Finally, a very similar relationship between the 3400 cm^{-1} peak's oscillator strength and the surface potential was also found, but the correlation was not quite as good.

Effect of Cations. To test for cation specific effects, VSFS measurements of the air/PNIPAM/aqueous interface were performed with various chloride salts. These included 1 M LiCl, 1 M NaCl, 1 M KCl, 1 M CsCl, 1 M $(CH_3)_4NCl$, 0.5 M $MgCl_2$, and 0.5 M $CaCl_2$. The spectra were essentially identical within experimental error (see Supporting Information, Figure S2). This suggests that the cations do not strongly associate with the PNIPAM interface and, hence, the interfacial water structure remains unchanged.

Ion Adsorption Isotherms and Gouy−Chapman−Stern Theory. The strong correlation between the surface potential and the 3200 cm^{-1} peak (Figure 6) affords a unique opportunity to measure the surface potential more accurately with VSFS than is otherwise possible with a Kelvin probe. As noted above, vibrating capacitor measurements are typically associated with a large degree of error.[45] The data in Figure 5 generally show increasing water signal with increasing salt concentration. To a first approximation, the concentration dependence for changes in the oscillator strength of the 3200 cm^{-1} peak can be fit by a simple Langmuir isotherm to abstract the corresponding fitting parameters (Table 1).

At a higher degree of scrutiny, however, changes in the surface potential (or the oscillator strength of the 3200 cm^{-1} feature) should not follow a simple Langmuir isotherm. This is

(50) Ong, S. W.; Zhao, X. L.; Eisenthal, K. B. *Chem. Phys. Lett.* **1992**, *191*, 327−335.
(51) Zhao, X. L.; Ong, S. W.; Eisenthal, K. B. *Chem. Phys. Lett.* **1993**, *202*, 513−520.
(52) Boman, F. C.; Musorrafiti, M. J.; Gibbs, J. M.; Stepp, B. R.; Salazar, A. M.; Nguyen, S. B. T.; Geiger, F. M. *J. Am. Chem. Soc.* **2005**, *127*, 15368−15369.

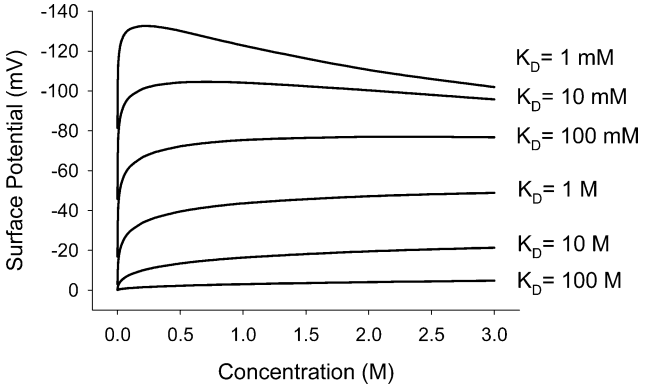

Figure 7. Concentration dependence of the surface potential predicted by Gouy−Chapman−Stern theory for anion adsorption. N_s is set at 5×10^{14} cm^{-2}. The solution is assumed to contain only the anion and its counterion, both of which are monovalent.

because Coulombic interactions between ions are significant and the Langmuir model does not take these into consideration. To account for Coulombic interactions, an extra electrostatic term can be introduced into the basic Langmuir model:[44,45]

$$\sigma_{ads} = \frac{zeN_s \frac{C}{K_D} \exp \frac{ze\varphi(0)}{kT}}{1 + \frac{C}{K_D} \exp \frac{ze\varphi(0)}{kT}} \quad (4)$$

Here, σ_{ads} is the surface charge density due to anion adsorption and z is the valence of the ion. C is the bulk ion concentration, N_s is the number density of binding sites, $\varphi(0)$ is the surface potential, k is the Boltzmann constant, T is temperature, and K_D is the equilibrium dissociation constant. The equation adopts the same mathematical form as the well-known Stern model.[44,45]

Equation 4 is not directly useful since it contains two unknowns: the surface charge density and the surface potential. According to Gouy−Chapman theory, a diffuse double layer is formed next to a charged plane in an electrolyte solution. This layer contains a net charge of opposite sign to the interfacial charge. The charge density in the diffuse double layer can be related to the surface potential and ionic strength of the bulk solution:

$$\sigma_d = (8I\epsilon_r\epsilon_0 kT)^{1/2} \sinh \frac{ze\varphi(0)}{2kT} \quad (5)$$

where σ_d is the net charge density in the diffuse double layer, I is the ionic strength, ϵ_r is the dielectric constant, and ϵ_0 is the permittivity of vacuum. To maintain neutrality, the surface charge, σ_{ads}, has to be balanced by the charge in the diffuse layer:

$$\sigma_d + \sigma_{ads} = 0 \quad (6)$$

Using eqs 4−6, the surface potential can be uniquely determined as a function of bulk ion concentration, assuming the solution contains no other salts. This relationship, however, cannot be written in a simple closed form. Instead, it must be determined numerically. Figure 7 plots the concentration dependence of the surface potential with K_D values varying from 0.001 to 100 M.

The concentration dependence of the surface potential is not a monotonic function. With increasing ion concentration, more ions adsorb and the greater surface charge density generates a greater surface potential. The surface potential, however, is not only determined by the surface charge, but also by the diffuse double layer, which acts as a screening layer. The screening effect also increases with ion concentration (ionic strength). The overall concentration dependence is a combination of these two competing phenomena.

At low concentration the surface potential rises in a nearly exponential fashion. This is mostly the result of Stern-type adsorption. At high concentration, however, the screening effect becomes dominant and the surface potential decreases roughly as the square root of the ionic strength. The competition between these two processes results in a maximum potential, the height and the position of which strongly depend on the value of K_D. The stronger the adsorption, the greater and earlier the maximum in the surface potential is found. However, the anions may not bind very tightly. This is the case represented by the bottom four curves in Figure 7. Under these circumstances, the maximum does not appear until very high concentrations, which may even exceed the solubility limits of the corresponding salt.

It should be noted that Gouy−Chapman−Stern theory is applied somewhat differently here compared with its common use.[44,45] In a typical system, ions adsorb onto a surface of opposite charge. This phenomenon is important only within the layer very close to the surface (the so-called "Stern layer"). Within the Stern layer, the potential drops rapidly as a function of distance from the surface. The surface potential is also lowered and the effect is stronger at higher ion concentrations. The screening effect with increasing ionic strength further reduces the surface potential, though at a slower pace. The surface potential, therefore, continuously decreases with increasing salt concentration in a standard system with an initial surface charge.

In the present case, the surface is initially neutral and the surface charge and the surface potential arise only because of ion adsorption. This is, therefore, not a "Stern layer" in the conventional sense, since the counterions have virtually no effect on this system. We still call the model Gouy−Chapman−Stern theory because the mathematical derivation is similar, though the concentration dependence of the system is different. An analogous case to the present system involves crown ether complexation in anion-exchange resins, whereby ion pairs are believed to be important.[53]

The oscillator strength/surface potential data from Figure 6 can be fit with the present theory and replotted in Figure 8. A single parameter, the equilibrium dissociation constant, is obtained from the fit to each ion. The agreement is excellent with the exception of sodium perchlorate. The K_D values for thiocyanate, iodide, nitrate, bromide, and chloride are 0.19, 0.50, 3.8, 4.0, and 15 M, respectively. These values are also provided in Table 1 as $K_{D,intrinsic}$ for the sake of comparison. The fits are better than the simple Langmuir fitting for the more chaotropic ions such as I^- and SCN^- (Figure 5). More significantly, the intrinsic dissociation constants are 6∼20 times larger (weaker binding) than the apparent dissociation constants obtained by Langmuir fitting.

For perchlorate, direct fitting with Gouy−Chapman−Stern theory is not completely successful. In this case a decrease in surface potential is found by 1 M (Figure 8, open circles, ○).

(53) Okada, T. *J. Phys. Chem. B* **1997**, *101*, 7814−7820.

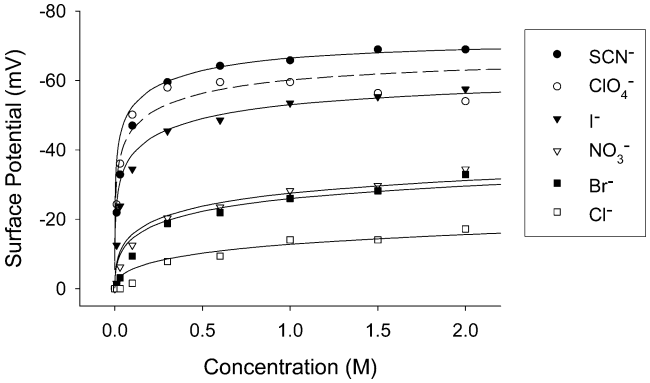

Figure 8. Changes in the surface potential as a function of salt concentration in the subphase. The lines represent fits using the Gouy−Chapman−Stern model. The fit for perchlorate is represented by a dashed line to emphasize the fact that it does not fit nearly as well.

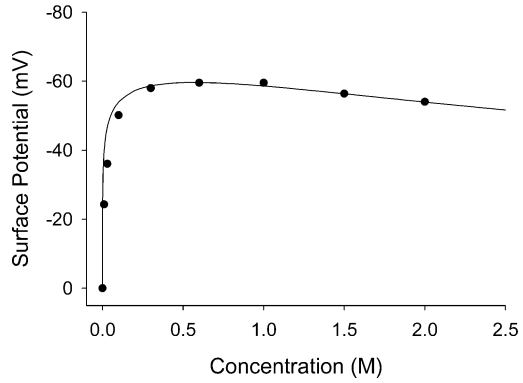

Figure 9. Change in surface potential as a function of $NaClO_4$ concentration in the aqueous subphase. The solid line is a fit to the modified Gouy−Chapman−Stern model from eq 5, 6, and 7.

This would suggest that perchlorate saturates the surface at relatively low concentration. It should be noted that perchlorate is much larger in size than the other chaotropic anions. If we assume that n sites are used for each binding event, then the Stern equation (eq 4) can be rewritten as follows:

$$\sigma_{\text{adsorption}} = \frac{zeN_s \frac{C}{K_D} \exp\frac{ze\varphi(0)}{kT}}{1 + n\frac{C}{K_D} \exp\frac{ze\varphi(0)}{kT}} \qquad (7)$$

Equations 5, 6, and 7 can be simultaneously solved in a numerical fashion to obtain the surface potential with this steric effect properly taken into account. Fitting the perchlorate data in this manner yields a dissociation constant of 0.15 M with an n value of 3.08 (Figure 9). This suggests that the adsorption of a single perchlorate ion blocks ~3 binding sites. Note that the dissociation constant for perchlorate is actually smaller (stronger binding) than the one found for thiocyanate. Indeed, perchlorate induces a more negative surface potential at low concentration (see Supporting Information, Table S2). Perchlorate, however, saturates much sooner because of the multisite blocking effect. Therefore, screening dominates at higher concentrations and results in an attenuation of the change in surface potential at concentrations around 600 mM $NaClO_4$. Without this steric effect, the screening effect would only become dominant over adsorption at extremely high concentrations. In fact, the apparent order of perchlorate and thiocyanate in the Hofmeister series is almost certainly reversed at low concentrations exactly because of this steric effect. This steric model may apply more generally and offer an explanation for the general observation that perchlorate and thiocyanate often switch their respective positions in the Hofmeister series.[2,37] It should be noted that subjecting the data from the other anions to this model generates n values very close to 1. This suggests that steric effects are not significant in those cases.

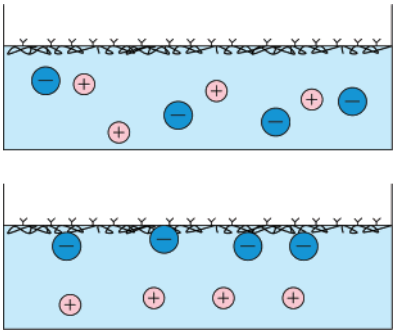

Figure 10. Anion adsorption onto PNIPAM at the air/water interface.

Discussion

Interfacial Water Structure in the Presence of PNIPAM Monolayers. It is generally believed that interfacial water orientation stems predominantly from local electric fields at the interface.[26,27] Previous studies have also shown that the water peaks increase in intensity as the surface charge density is increased.[34−36] For PNIPAM spread on a pure water subphase, only very weak OH-stretch peaks were observed from the uncharged layer (Figure 2b). When chaotropic anions were introduced, however, the water peaks became much more prominent. For example, the 3200 cm^{-1} peak was approximately 2 orders of magnitude more intense in the presence of 1 M NaSCN than on a pure water subphase (Figure 4).

It should be noted that the results from the PNIPAM interface stand in stark contrast to other common systems. In typical cases, adding salt into the subphase screened the electric field and weakened the OH-stretch peaks in corresponding VSFS spectra.[34−36] The difference here is that the adsorption of the anions are directly responsible for creating the interfacial potential (Figure 10). Moreover, the degree of interfacial water orientation at a given salt concentration was found to depend directly on an anion's position in the Hofmeister series (Figure 3a). On the other hand, varying the cations appeared to have little if any effect. These observations are generally consistent with the notion that weakly hydrated ions can shed their hydration shells and associate with the interface, while more strongly hydrated ions cannot.[54]

The linear correlation between the surface potential and the oscillator strength of the 3200 cm^{-1} peak appears to suggest that the relationship between surface charge and water alignment is direct (Figure 6). The drop in surface potential found in the vibrating capacitor experiments should correlate with water dipole moments aligning away from the surface (hydrogen atoms up, oxygen atoms down). Indeed, the interference between the OH and CH stretches is constructive (comparing Figure 3a and Figure 3b), similar to other systems with a negative charge.[29,30,33−36]

(54) Marcus, Y. *Ion Properties*; Marcel Dekker: New York, 1997.

In fact, the most chaotropic anions gave rise to the greatest VSFS intensity between the CH- and OH-stretch regions (∼3000 cm^{-1}).

Adsorption behavior can be viewed as a partitioning of the anions between the interface and the bulk solution. The equilibrium constant and the bulk concentration dictate the distribution between these two states. For an anion to be adsorbed at the interface, it needs to undergo partial desolvation. The chaotropic anions have relatively low solvation free energies mostly because of their generally large size and high polarizability.[54] Therefore, a smaller desolvation penalty is paid compared with the kosmotropic anions. We believe that this is the major reason for the specific anion effects seen in this system. Recent calculations and experiments have shown that chaotropic anions are concentrated at the air/water interface in a trend which is also consistent with the Hofmeister series.[17−21] In addition, the generally greater polarizability of chaotropic anions may also facilitate adsorption through direct interactions with PNIPAM's amide dipole.[9−11]

It is of great interest to compare the phenomena observed in the present system with related experiments that also show specific ion effects at aqueous interfaces. For example, air/water interface studies of sodium halide solutions have been conducted with VSFS in several laboratories.[23,55,56] In those cases it was also found that anions were enriched in the uppermost layer at the interface, relative to cations.[21] Moreover, the most chaotropic halides had the greatest preference for the interface. A key difference, however, between the air/solution interface results and the present data is the magnitude of the specific ion effect. Namely, the specific ion effects are much more pronounced for the polymer interface. For example, the water peak induced by iodide at the air/PNIPAM/aqueous interface is ∼100 times stronger than at the air/water interface. Indeed, chaotropic anions should partition much more readily into a hydrated polymer than into a bare air/water interface.

A previous study by our laboratory investigated specific ion effects on octadecylamine (ODA) monolayers at the air/water interface.[8] In that case the Langmuir monolayer bore a partial positive charge, and the water signal was attenuated as salt was added to solution. Different anions attenuated the signal to different extents; however, no clear correlation could be found between the Hofmeister series and the degree of water orientation. It should be noted that the interactions between the anions and the monolayer involved electrostatic interactions with the positively charged head groups of ODA. Such interactions affected the surface density of the ODA molecules, the alignment of their fatty acid chains, and the net charge at the interface. All these effects, in turn, influenced interfacial water structure and orientation. By contrast, the PNIPAM monolayer in the present case has relatively less complex interactions with the anions. In fact, Figure 3b indicates that the orientation of the PNIPAM layer was nearly unaffected by the presence of various salts in solution. Therefore, the largest influence of the anions comes from the modulation of the surface charge density. The degree of interfacial water alignment follows the Hofmeister series for the air/PNIPAM/aqueous system simply because the interactions between the anions and the macromolecule directly follow this series. This implies that the underlining mechanism of interfacial water structure ordering is not directly affected by the identity of the anion dissolved in the subphase, but merely a consequence of polymer−ion interactions.

Biophysical Implications. Hofmeister salts can bind to biomacromolecules and induce the alignment of adjacent water molecules. For example, proteins near their isoelectric point would be expected to have their adjacent waters aligned (and surface potential modulated) according to the Hofmeister series as various salts are added to solution. Such changes should be important in many phenomena, such as protein solubility, aggregation, denaturation, and related protein−protein interactions.

Acknowledgment. We thank the National Science Foundation (Grant CHE-0094332) and the Robert A. Welch Foundation (Grant A-1421) for funding. We also thank Prof. David E. Bergbreiter for providing the PNIPAM sample.

Supporting Information Available: VSFS spectra of PNIPAM on subphases at various pH values, the introduction of various cations to the subphase, surface potential measurements, and fitted oscillator strength values. This material is available free of charge via the Internet at http://pubs.acs.org.

JA073869R

(55) Schnitzer, C.; Baldelli, S.; Shultz, M. J. *J. Phys. Chem. B* **2000**, *104*, 585−590.
(56) Raymond, E. A.; Richmond, G. L. *J. Phys. Chem. B* **2004**, *108*, 5051−5059.